CHAPTER- 1

* INTRODUCTION *

1.1 Structure Of the Neutral Thermosphere and the Ionosphere

The earth's atmosphere consists of various gases in different proportions. The overall gas density near the surface of the earth is ~ 10^{19} particles cm^{-3} and it decreases exponentially with height. In the presence of gravity, it is horizontally stratified into different layers or regions. Based on the altitude variations of neutral temperature, the earth's atmosphere is classified into the troposphere (0-15 km), the stratosphere (15-50 km), the mesosphere (50-90 km) and the thermosphere (90-400 km). The boundaries separating each of the above mentioned 'sphere' are the tropopause, stratopause and mesopause respectively . The altitudinal temperature structure shows a decrease initially from 270° K up to tropopause (170° K) due to decrease in the infrared radiation's from the earth. Later, an increase in temperature is seen up to stratopause (260° K) owing to the absorption of solar UV-radiation by ozone layer. The temperature reaches a minimum value at the mesopause region (150° K) essentially due to radiative cooling. Above this region i.e. in the thermosphere, there is a steep temperature gradient and it reaches a maximum in the range of 600-1900° K, depending on the solar activity levels. The dense lower and middle atmosphere (up to 90 km), is dominated by turbulence due to which all the species are homogeneously

(well) mixed and is called the 'homosphere'. Above this altitude, vertical mixing is inhibited since the temperature rises with height making the atmosphere more stable. On the other hand, molecular diffusion dominates in this region aided by less number of collisions and hence each kind of species is distributed on its own according to its molecular weight. In the absence of chemistry, the gases exist essentially in the diffusive equilibrium. Due to its varying composition with height, this region is called the "heterosphere". The boundary separating the homosphere and the heterosphere is called as "turbopause". The distribution of various species with respect to height along with the above mentioned regions and is shown in fig. 1.1. There exists further, a broad classification of the atmosphere, mainly based on the differences in the dominant physical processes, which are sensitive to different observational techniques. The region between 0-15 km is called the "lower atmosphere", the region between 15-90 km is the "middle atmosphere" and the region above 90 km is referred to as the "upper atmosphere".

The region of our interest lies in the upper atmosphere, i.e. the thermosphere, where the temperature starts rising from the base (90 km) to reach a constant value about 350 km altitude region. Its upper boundary is rather ill-defined. Within the thermosphere the various gases are in thermal equilibrium with each other and fluid dynamic principle is valid in this region.

The structure and dynamics of the upper atmosphere, in general,

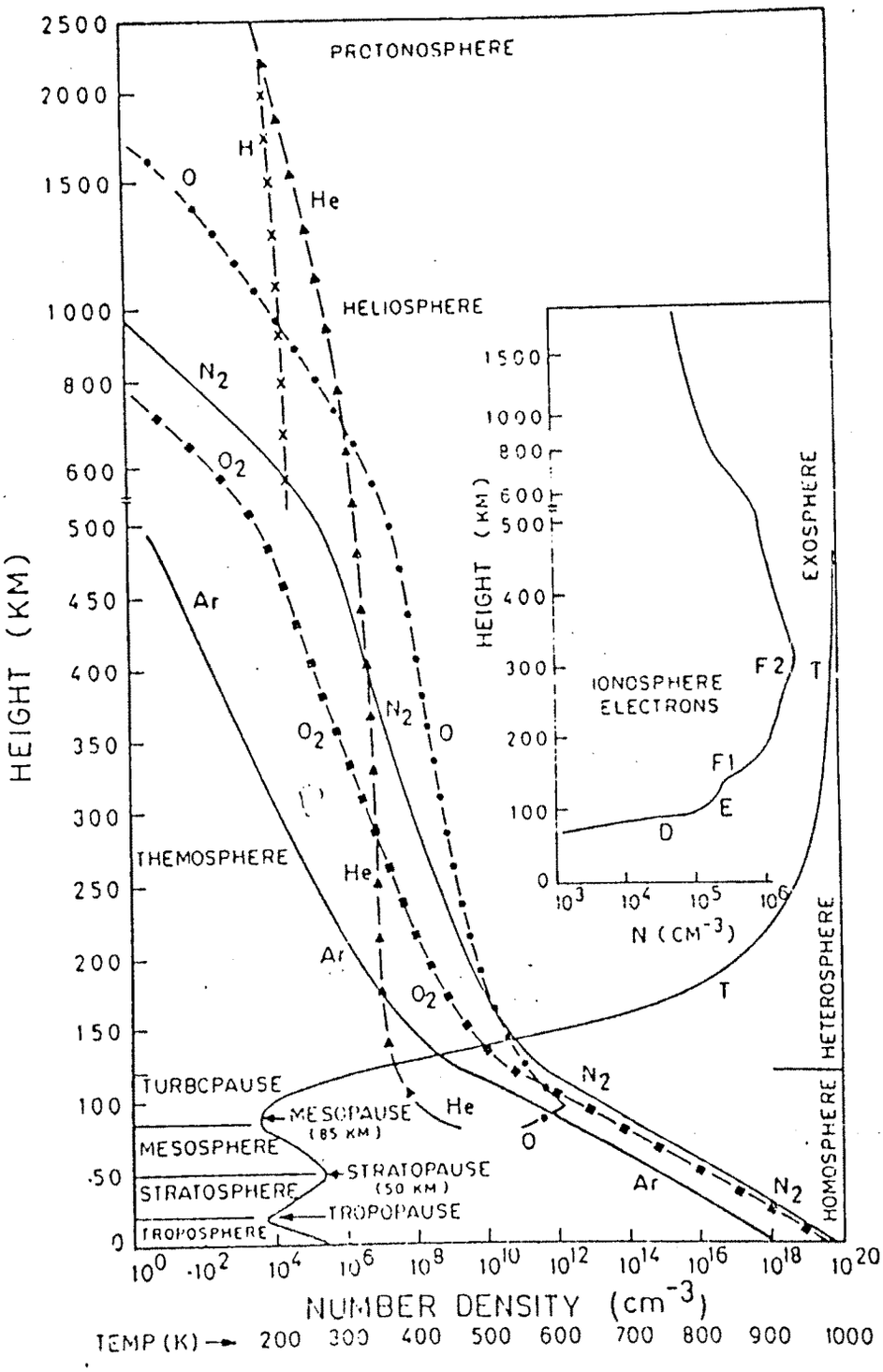

Fig.1.1. The earth's atmospheric structure showing various regions, distribution of neutral species and temperature. The inset shows the height distribution of the ionized species.

are mainly governed by the different forms of the solar energy input into the atmosphere, Viz: (1) the characteristic black-body radiation of the sun, (2) the solar wind, and (3) the solar X-ray and UV radiation that are mainly responsible for the formation of the ionosphere.

The solar wind which consists of protons of ~1 keV energy and almost equal number of electrons with energies of few-hundred eV. Apart from directly depositing energy into the atmosphere, confines the geomagnetic field lines to ~ 10 R_E on the dayside and stretches the same to > 100 R_E on the nightside. The inputs into the atmosphere at the equatorial and low latitudes are mainly through the UV and X – radiation, at high latitudes, particles of solar wind origin deposit, on the average, comparable amount of energy to the atmosphere.

The thermosphere is a multi-constituent medium made up of molecular nitrogen (N_2), atomic and molecular oxygen (O,O_2) as major gases and little amount of Argon and Helium among other species. The interaction of solar ultraviolet radiation with constituents of the thermosphere, triggers a host of chemical reactions and produces electron-ion pairs, and causes dissociation of chemically active molecular oxygen.

Due to the varying chemical composition with altitude, different ionization layers are produced within the thermosphere and mesosphere, depending on the dominant absorbing species. Thus atomic oxygen, which is more in number than other gases above 150 km produced as a

result of photodissociation of O_2, gets ionized and forms the F-region. The composition below this region is mainly molecular and the ions such as O_2^+ and NO^+ constitute to form the E-region whose base at 90 km. The ionization below the E-region is called as D-region. At the altitude above 900 km hydrogen ions become the dominant and is called the protonosphere. The ionosphere is thus, the plasma with equal number of positive ions and electrons , that can affect the propagation of radio waves. During daytime, distinct 'layers', like the E - layer, F_1 - layer, F_2 - layer with increasing ionization are formed and is shown in Fig-1.2.

The main source of heat for the neutral upper atmosphere is the absorption of UV and EUV radiation from the absorption from the sun by these species. This heat input and the downward conduction of it governs the temperature structure of the upper atmosphere, giving rise to a steep gradient in the altitudinal temperature profile from ~ 90 km to around 300 km. Above 300 km, the thermal conductivity is high and the isothermal condition exists. Much above this region (~1000 km) atmospheric species have sufficient kinetic energy to escape the gravitational force of the earth. This region is referred to as the "exosphere" and the corresponding temperature is known as the exospheric temperature, T_∞. Satellite measurements have shown that there is a diurnal variation in this temperature with maximum and minimum values at ~1600 hrs LT and 0300 hrs LT respectively **[1].**

The ionosphere shows a large diurnal variability in addition to solar

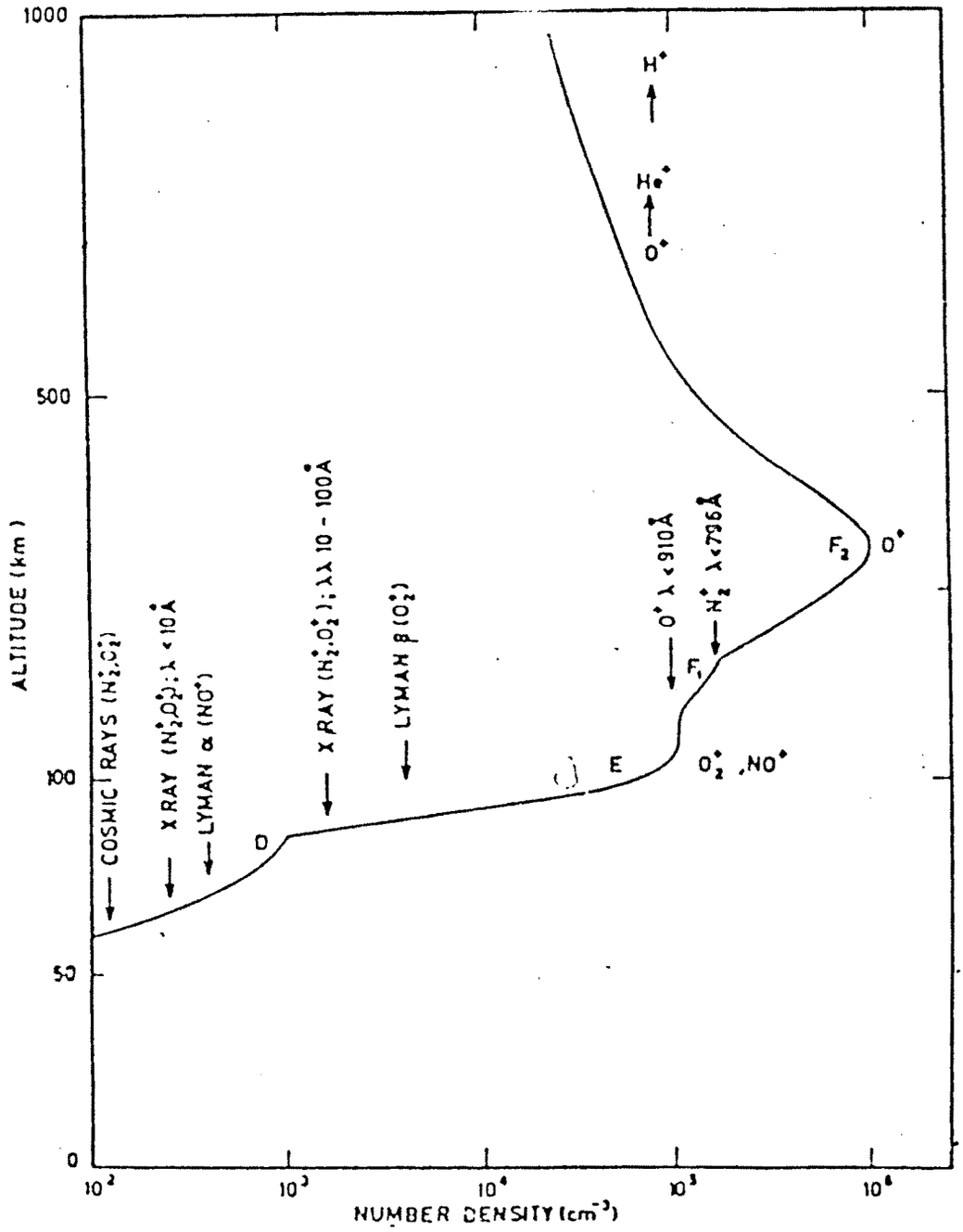

Fig.1.2. Average daytime electron density distribution with height. The principal ions in each region and the corresponding ionizing radiation are indicated.

cycle variations and the typical altitude profiles of densities in day and nighttime are shown in figures 1.3 (a),(b).In the D-region ion and electron motions are controlled by the neutral winds and turbulence owing to their high rate of collision with neutrals .The E-region of ionosphere, also referred as the dynamo region is formed mainly due to photo-ionization by EUV in the wavelength range of 911-1027 A° **[2]** .Here the motion of the ion is controlled by the neutral winds owing to their collision frequencies with neutrals (ν_{in}) being higher as compared to their gyrofrequencies (Ω_i) . Whereas, the electrons are confined to move along the magnetic field lines as their gyrofrequencies (Ω_e) are larger as compared to their collision frequencies with the neutrals (ν_{en}).

The F_1-region can be considered to be extending above 140 km and photo-ionization is due to the EUV radiation between 170-911 A° and also the He-I and He-II lines, at 304 A° and 984 A° respectively, in the solar spectrum. The peak production of F-layer lies at around 150 km for vertically incident solar radiation .The production rate above this height is limited by the available neutral species while below the height by the available solar flux and is shown in Fig-1.4. The peak production height goes up with increase in solar zenith angle.

1.2 The Energy Balance of the Thermosphere

The energy input in the form of UV and EUV radiation from the sun, are responsible for the large temperature in the thermosphere. This

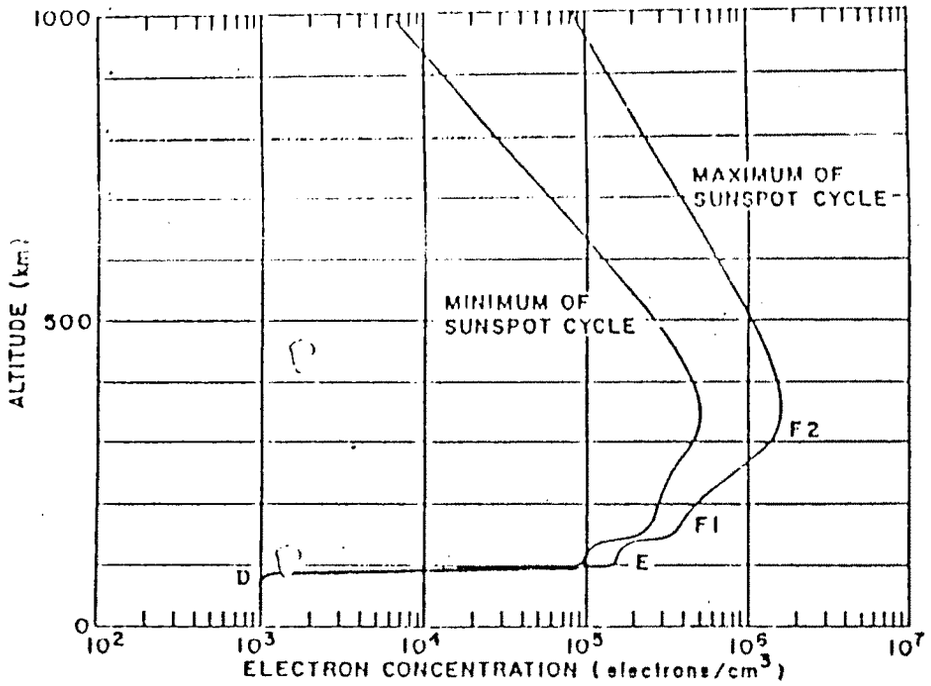

a. Daytime.

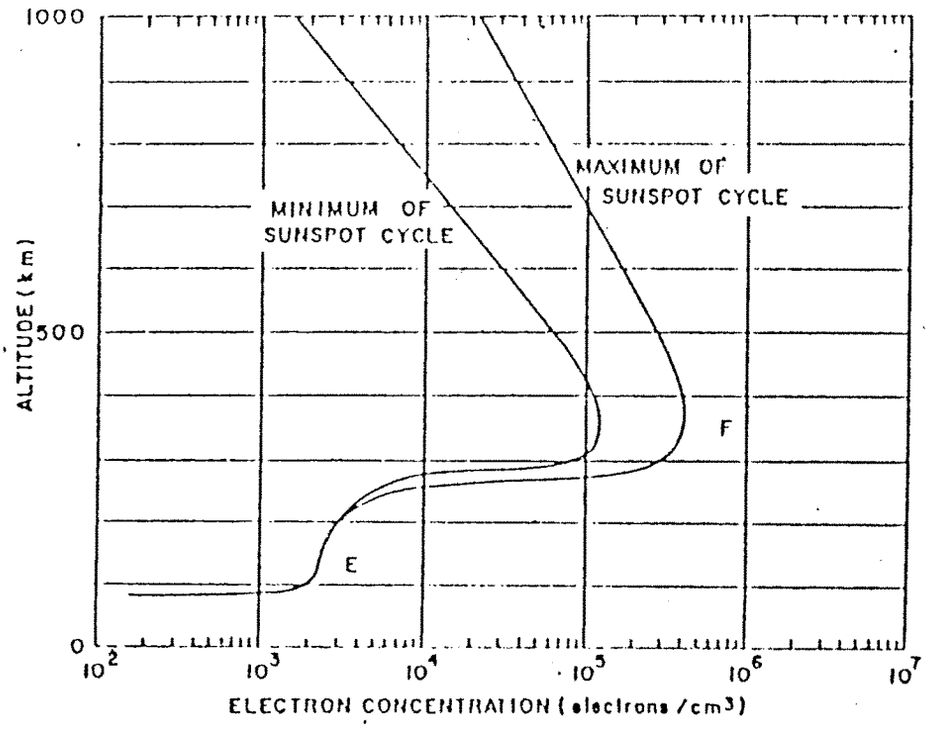

b. Nighttime.

Fig.1.3. Electron density distribution with respect to solar epoch during (a)daytime and (b) nighttime.

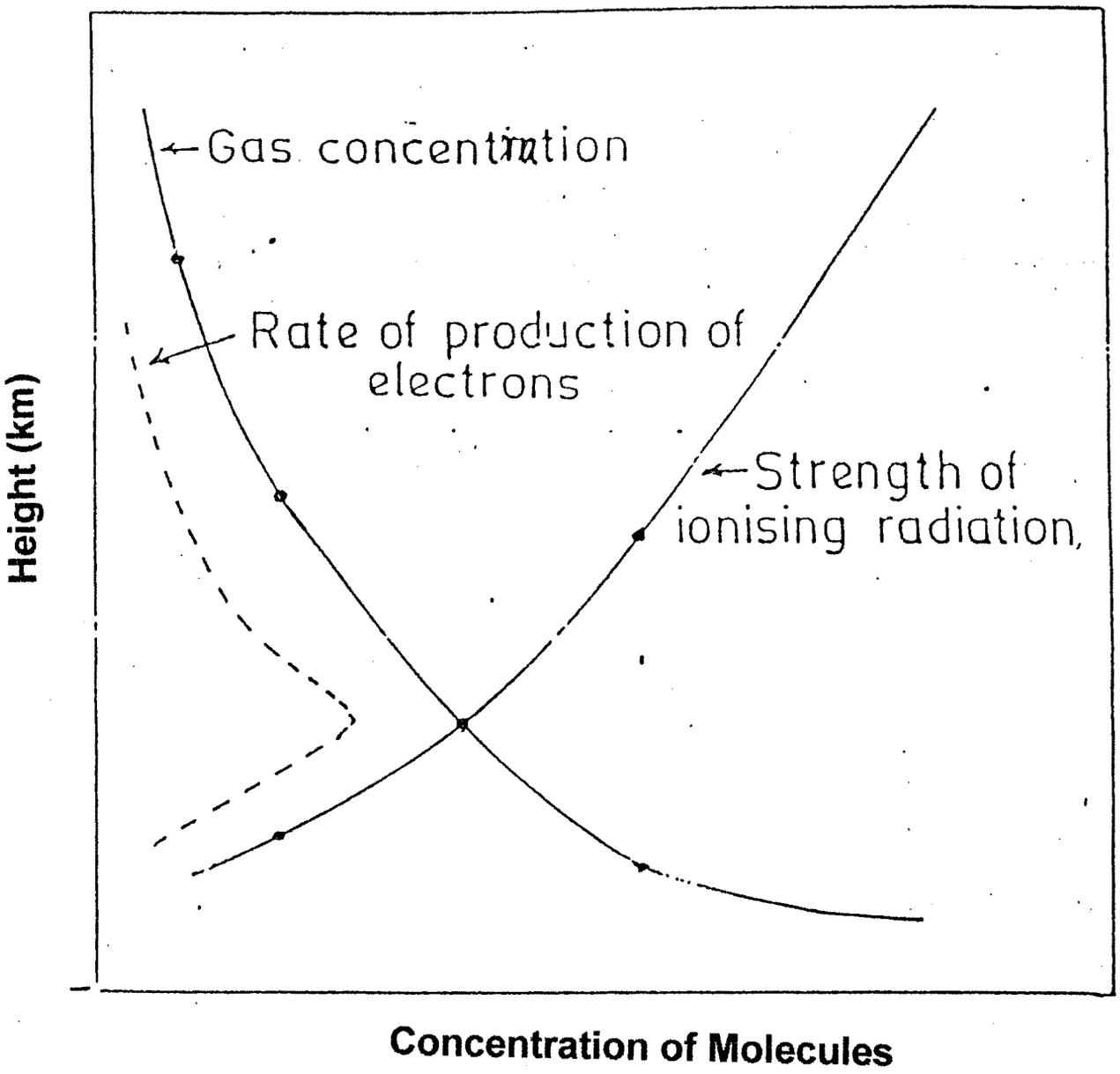

Fig.1.4. This shows the formation of ionosphere due to interaction between ionizing radiation of sun and neutral atmospheric constituents.

energy is transferred to the various atmospheric gases by means of photochemical process. At high latitudes, Joule dissipation of electric currents driven by electric fields of magnetospheric origin and energetic particle precipitation, essential during a geomagnetic storm, also contributes to the heating of thermosphere. On a global basis, heating by various sources is balanced by the downward thermal conduction and the radiative cooling by species such as nitric oxide, and results in the observed thermal structure.

The interaction of solar radiation with thermospheric species gives various paths by which the energy is channeled into heat. The ejected primary photoelectron after a photoionization carries the excess energy and undergoes Coulomb collisions with ambient electrons and ions, and inelastic collision with the neutrals. The most of photoelectron energy is lost to space by means of airglow emissions that results from excitation of neutrals. The remaining part is used to heat the neutral gas with an efficiency of about 5%. The combined neutral gas heating efficiency for both ion photoelectron channels is estimated to be in 30-40% range **[3].**

The neutral gas above 300 km, is heated by collision with the hot electrons and ions. Below this altitude up to ~170km, the thermal energy is provided by photoelectrons and exothermic chemical reactions. The photo-dissociation of O_2 by the Schumann-Runge continuum (1250-1750 A°) of solar radiation is the dominant heat source below 170Km with 30% efficiency. The path along which the solar EUV energy gets channeled to

ultimate heating the neutral thermosphere is shown in Fig-1.5.

The uneven absorption of solar energy over the different regions of the atmosphere generates pressure gradient on a global scale, which drives neutral air circulation. The neutral winds redistribute heat by transferring energy from warmer dayside toward the cooler nightside of the thermosphere. Further, inhomogeneities in ionization densities produces drag effects on the neutral air motion that may lead to localized heating and associated circulation **[4].**

During geomagnetic storms precipitation of energetic neutrals can also be a direct source of heat for equatorial region , produced through charge-exchange reaction with the ring current ions **[5].** However, the heating of the thermosphere due to this source is yet to be quantified. During enhanced geomagnetic activity, energy is transferred from high latitudes to equatorial and low latitude regions by means of dynamic processes **[6].**

Upward propagation of tides and gravity waves generated in the lower and the middle atmosphere is also important in the global energy budget since their dissipation due to molecular viscosity, thermal conduction and frictional interaction with ions yields significant energy **[7 - 10].** An excellent and more recent review on the global energy balance of thermosphere taking into account the various sources and sinks, exists in the literature **[11].**

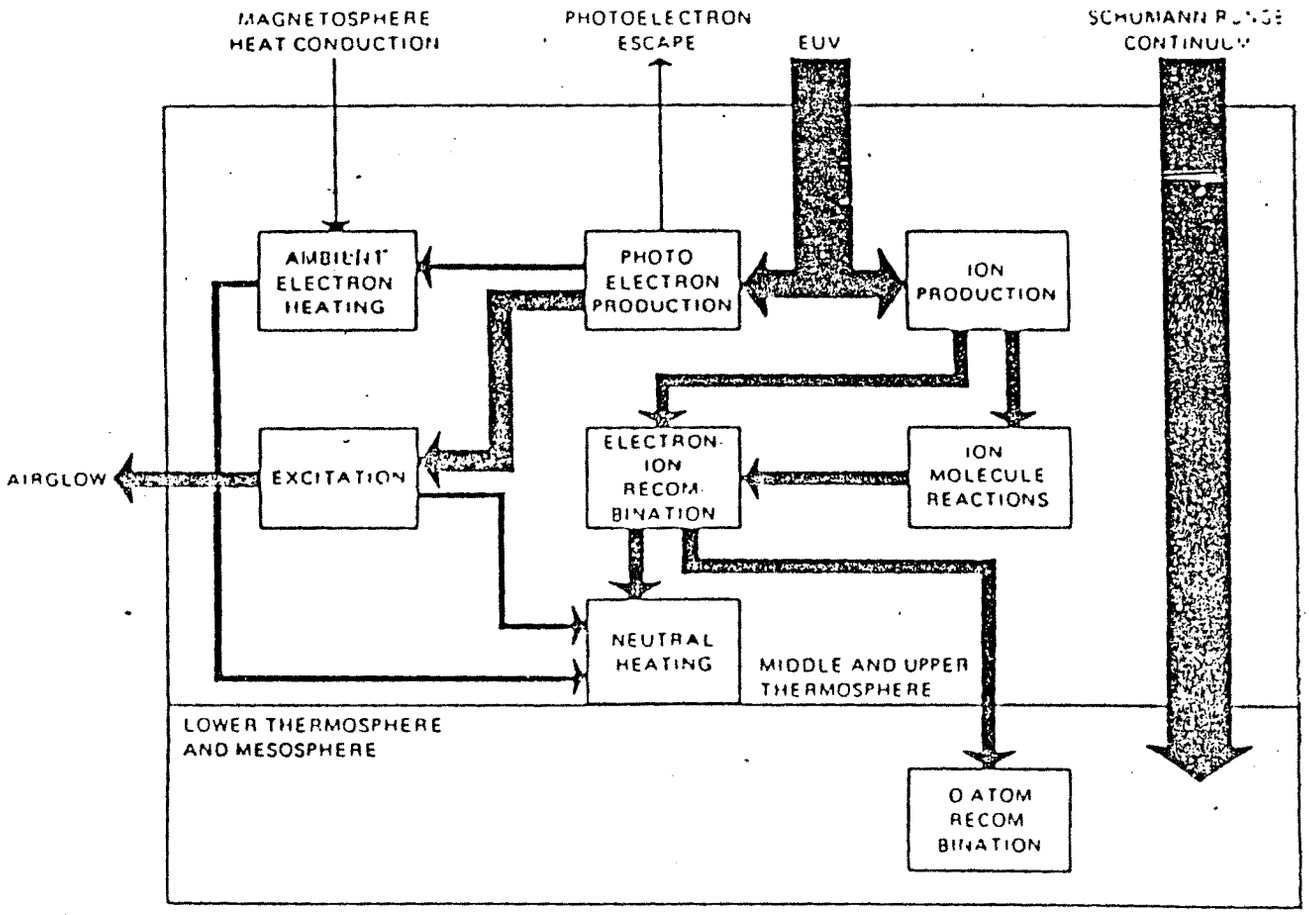

Fig.1.5. Energy flow diagram of the processes that lead to the conversion of absorbed solar EUV radiation into local thermal energy of neutral gas. The width of the arrow indicates the relative energy in each process.

1.3 Upper Atmospheric Phenomenon

All, the upper atmospheric phenomenon are essentially due to the dynamical variations in this region. The differential heating of the upper atmosphere by solar UV and EUV radiation sets in a variety of transport processes, the complete understanding of which is essential for the study of structure, energetic and dynamics of the atmosphere. The solar EUV is the main source of heat to the equatorial and low latitude thermosphere, particles of solar wind origin account for heating of the high-latitude thermosphere to a great extent. The heating is both via Joule dissipation due to the intense auroral currents **[12]** and also due to interparticle collisions. Moreover, there are other means, such as the atmospheric waves and tides, planetary and acoustic waves, gravity waves, etc which originate in the lower atmosphere and as they propagate to higher altitudes, give rise to heating in the upper atmosphere due to wave breaking into turbulence. The non-uniform absorption of solar energy by different regions of the earth gives rise to pressure gradient, which sets large-scale wind motions. These are good carriers of thermal energy and momentum, also plays an important role in the energy redistribution. In thermosphere the main operative wind systems are the diurnal winds from dayside to nightside and the prevailing wind form hot summer hemisphere to cooler hemisphere fig-1.6 .The solar tides are mainly responsible for the global scale dynamo action in E-region generating electric fields. The interaction of such electric fields, tides, winds etc., in the presence of

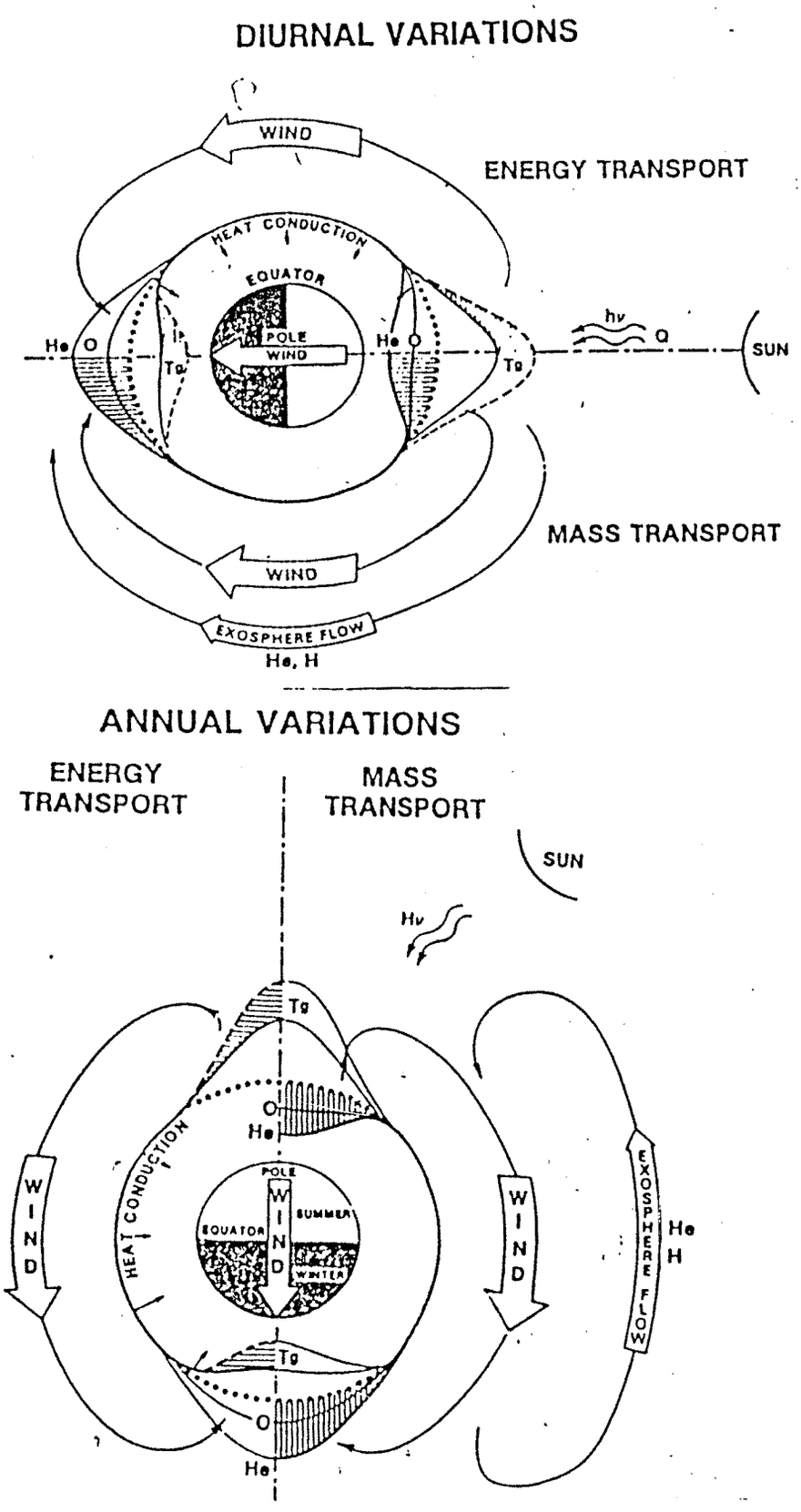

Fig.1.6. Schematic illustration of diurnal and annual tides.

geomagnetic fields gives rise to the earth's upper atmosphere. These are discussed in the following section.

1.3.1 Equatorial / Low-latitude Phenomena

(A) Equatorial Electrojet (EEJ)

In 1724, *Graham* reported that the earth's magnetic field undergoes daily variations. Later, in 1882, *Belfour Stewart* **[13]** interpreted these variations as due to thermally forced motion of electrically conducting air moving across the earth's magnetic field in the upper atmosphere. The effect of global scale tidal winds maximizes in the E-region, where the ion moves along the neutral winds but the electrons are confined to the magnetic field lines. This is analogous situation to a dynamo resulting in the generation of electric fields. These electric fields over the dip equator are in the east-west direction. The eastward field crosses with the northward magnetic field giving rise to an $\mathbf{E} \times \mathbf{B}$ drift and only electrons which are constrained to the magnetic field lines respond to it as ions are tide up with neutrals. The resulting polarization field is directed vertically upward (Hall direction), in turn, crosses with the magnetic field to give rise to an enhancement in the electrical conductivity (cowling conductivity) and results in an intense band of current in a narrow ($\pm 3°$) region, very close to the dip equator. This narrow latitudinal band of strong eastward electric current centered near 106 km over the dip equator in the E-region with a peak current density around noon-time, is referred to as the equatorial electrojet (EEJ). Fig. 1.7 shows the variation of the horizontal component

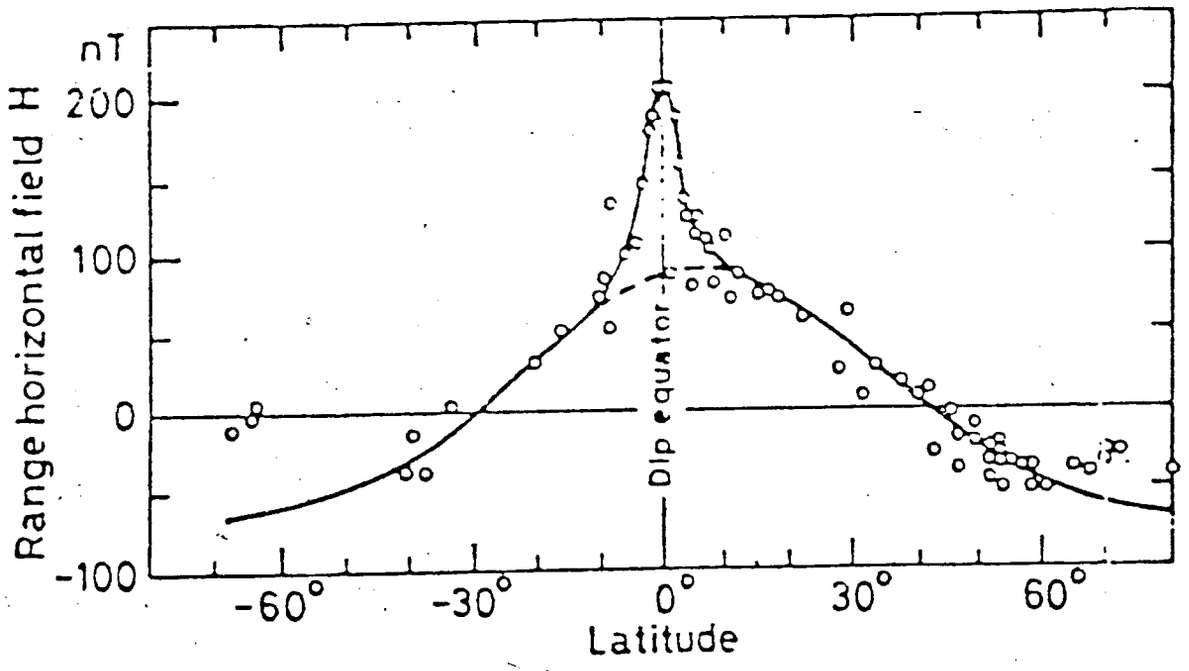

Fig.1.7. Variation of the horizontal component of earth's magnetic field at noon over various latitudes.

of earth's magnetic field at noon over various latitudes. The east-west electric field is about 0.5 mV/m and the vertical field 10 mV/m. The current flows eastward by the nighttime section is less evident because the electron density is smaller by night. The in-situ measurement by rocket shows the height of the peak current density is to be around 106 km **[14]** and thickness to be 15-20 km.

In the Indian longitudes, the strength of the EEJ is estimated from the difference of the magnitudes of the horizontal component of magnetic field between Trivandrum ∇H_T (0.2°N dip lat.), a station under the electrojet belt and Alibag ∇H_A (13.2°N dip lat.), a station well away from it. The polarity of this field is usually westward from sunset to sunrise times. It has been observed on some occasions that the polarity of electrojet reverses in the day time itself for a short duration and this phenomena is called the counter-electrojet (CEJ).

(B) Counter Electrojet (CEJ)

On some occasions the daytime ∇H values at the equatorial region go beyond the mean nighttime field strength and these are termed as counter-electrojet (CEJ) **[15--17]** (shown in Fig-1.8). During lower solar activity periods the CEJ shows larger frequency of occurrence. The reason for the occurrence of such large westward-directed electric currents in the noontime is still unsolved problem. *Raghavarao and Anandrao* **[18]** and *Anandrao and Raghavarao* **[19]** hypothesized the CEJ may be due to the vertical winds of gravity wave origin.

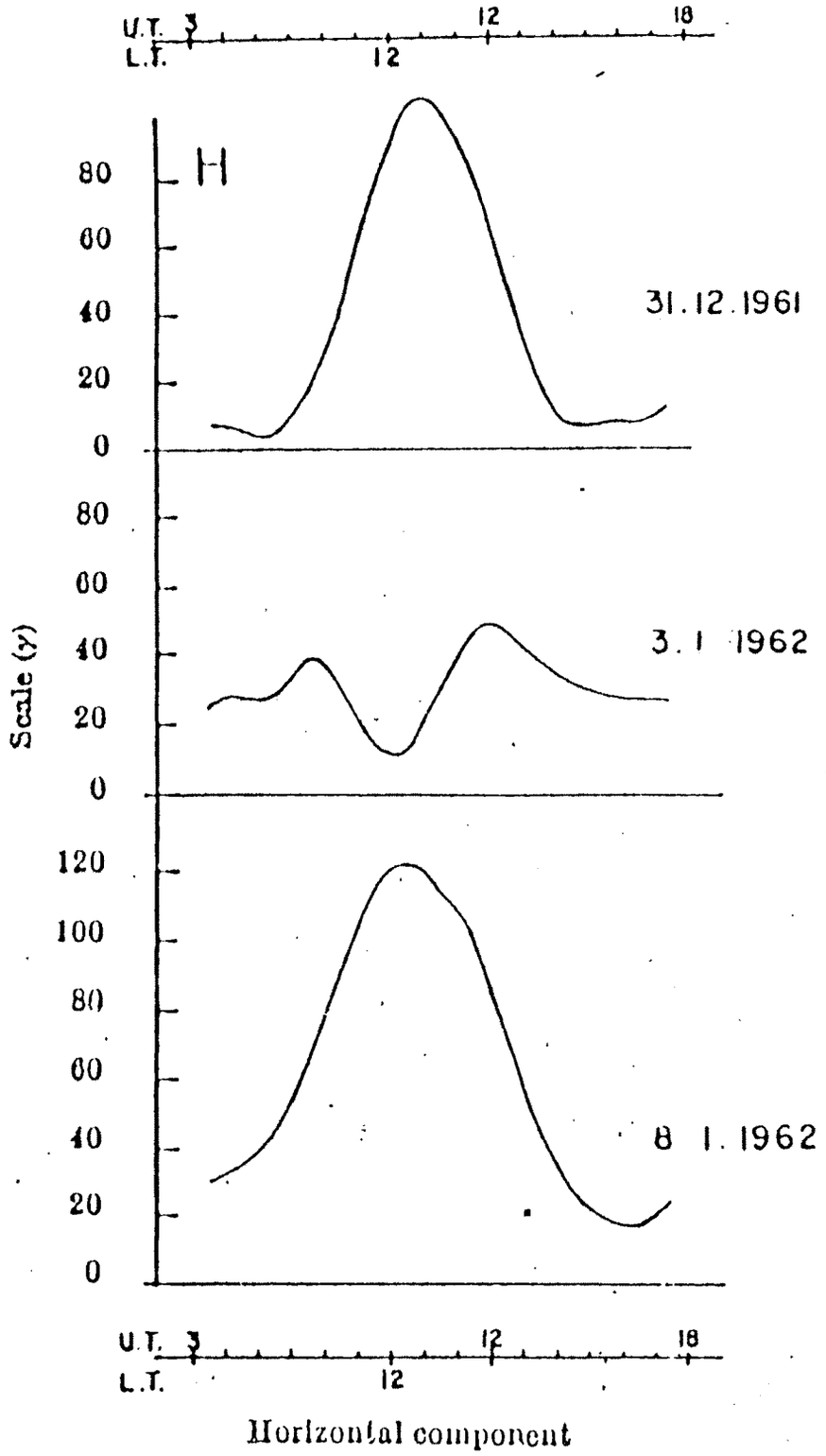

Fig.1.8. Variation in electric field over a dip equatorial station, Addis Ababa, during the counterelectrojet events. (*After Gouin*,1962).

(C) Fountain Effect

The day-time F-region electric field is controlled by a delicate balance between production of ionization through photoionization and loss due to chemical and plasma transport processes. In the vicinity of dip equator, vertical diffusion of plasma takes place with the imposition of an electric field because of unique configuration of geomagnetic field in this region. Such an electric field originates due to global E-region dynamo driven by tidal winds. The E-region east-west electric field gets mapped to the F-region through the highly conducting geomagnetic field lines and controls the plasma movement in the vertical direction through $\mathbf{E} \times \mathbf{B}$ drift. In addition, the gyrofrequency is much larger than the ion-neutral frequency at F-region heights, the plasma once lifted upwards can diffuse along the geomagnetic field lines under the influence of pressure and the gravitational gradient forces. Usually during the nighttime, the electric field reverses in direction and becomes westward and as a result the plasma moves equatoward which is known as reverse ionization anomaly.

(D) Equatorial Ionization Anomaly (EIA)

The fountain effect is responsible for the equatorial ionosphere's best-known anomaly, the 'Appleton' anomaly or simply the equatorial anomaly, shown in Fig.1.9. Instead of the electron density coming to maximum over the equator, as we might expect, there is actually a minimum over the magnetic equator. Topside and bottomside ionogram shows that the separation between the peak depends on the height and

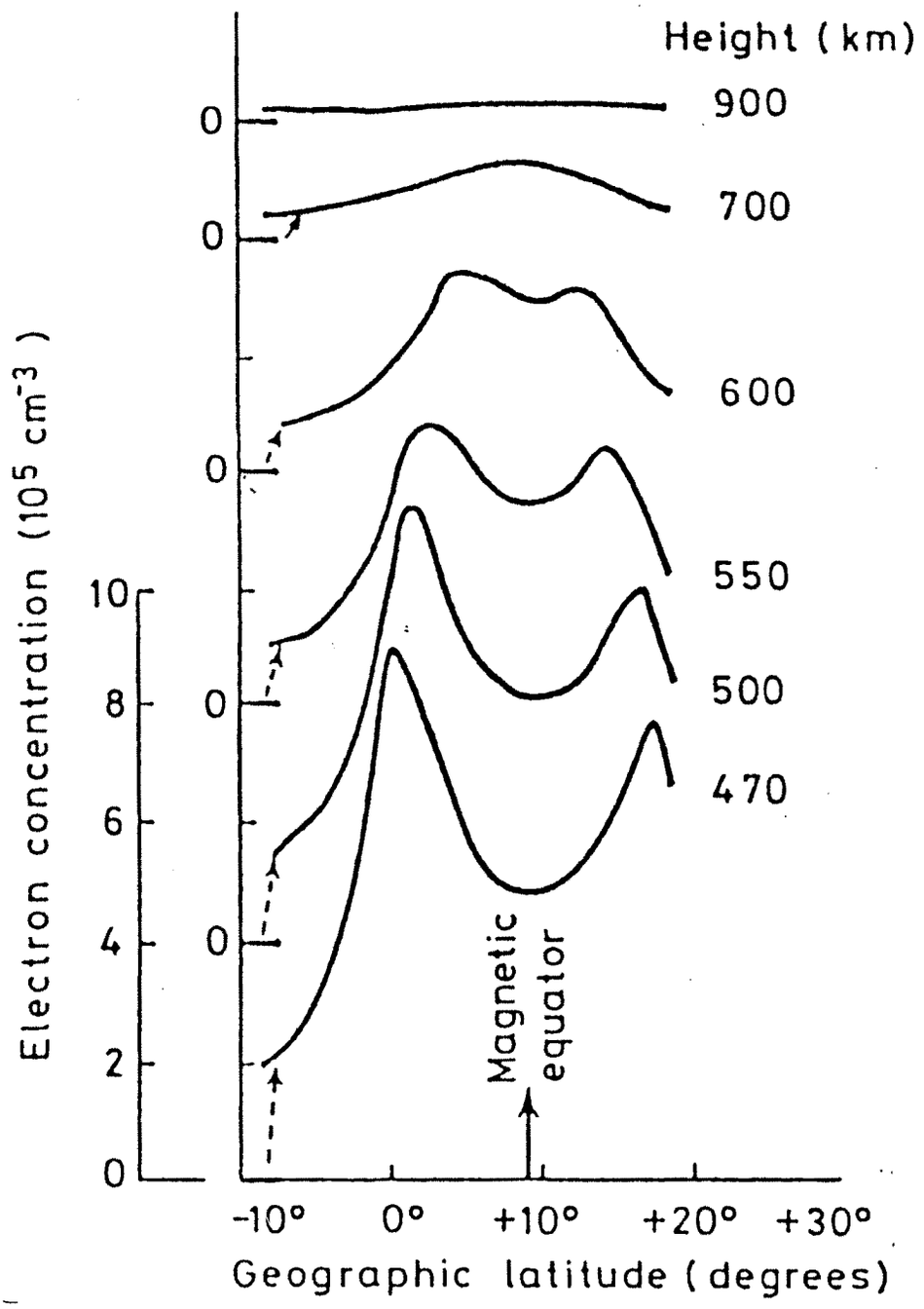

Fig.1.9. Equatorial anomaly.

they tend to merge at about 500-600 km. One of the classic representation of the EIA has been presented by *Croom et al* **[20].** Wherein they showed the anomalous electron density distribution during noontime, at different heights, with respect to various latitudes along a longitude sector using a chain of ionosonde (Fig.1.10). In addition to the day-to day variability, EIA exhibits a strong seasonal and solar cycle dependence **[21- 24]** as well as longitudinal dependence **[25-28].** This phenomenon is an excellent example of the E-and F-region coupling as the integrated strength of the electrojet (up to noontime) shows nearly 100% correlation with the EIA strength **[29].** Many reviews on the equatorial ionization anomaly exist in the literature **[30- 32].**

(E) Neutral Anomaly (NA)

Near the equator, the atmospheric structure and dynamics are much more complicated. *Hedin and Mayer* **[33],** from the OGO-6 satellite data, presented latitudinal and longitudinal variations of N_2 density. They showed about 20% enhancement (crest) at ~± 17° dip latitude and trough over dip equator (and not over geographic equator) during 1700 hrs LT, while in the morning (at ~06:00 hrs LT) the N_2 densities maximized over the dip equator. This anomalous behavior of neutrals revealing a geomagnetic control in their latitudinal distribution is called the "neutral anomaly" (NA) (Fig.1.11). The anomaly may be due to the ion-drag experienced by the neutrals due to plasma. Which diffuses along the field lines as consequences of the development of EIA crests, as compared to

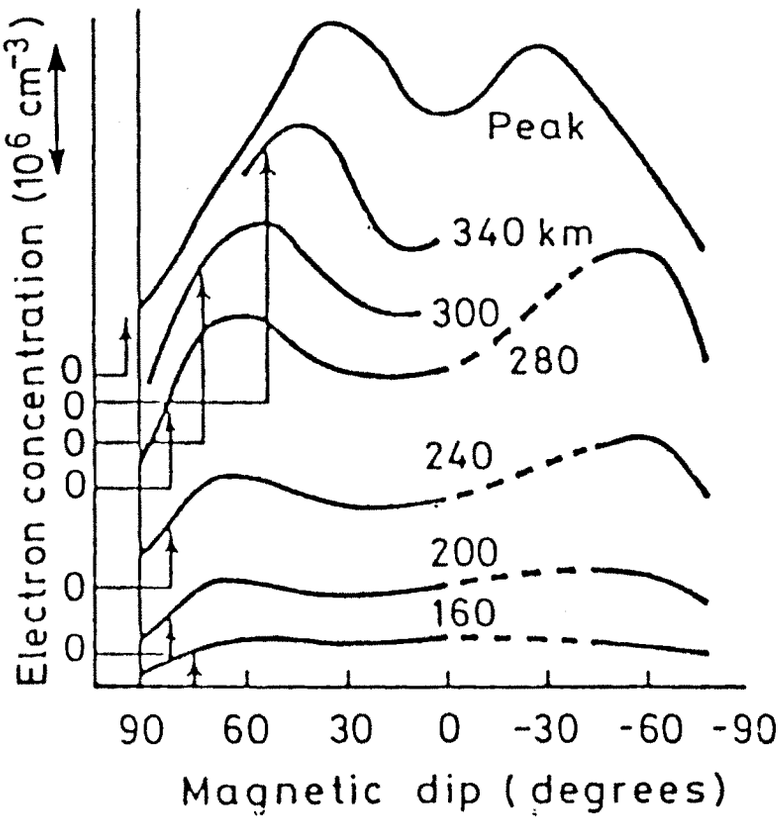

Fig.1.10. Distribution of electron densities at noontime at different heights along the longitudes.

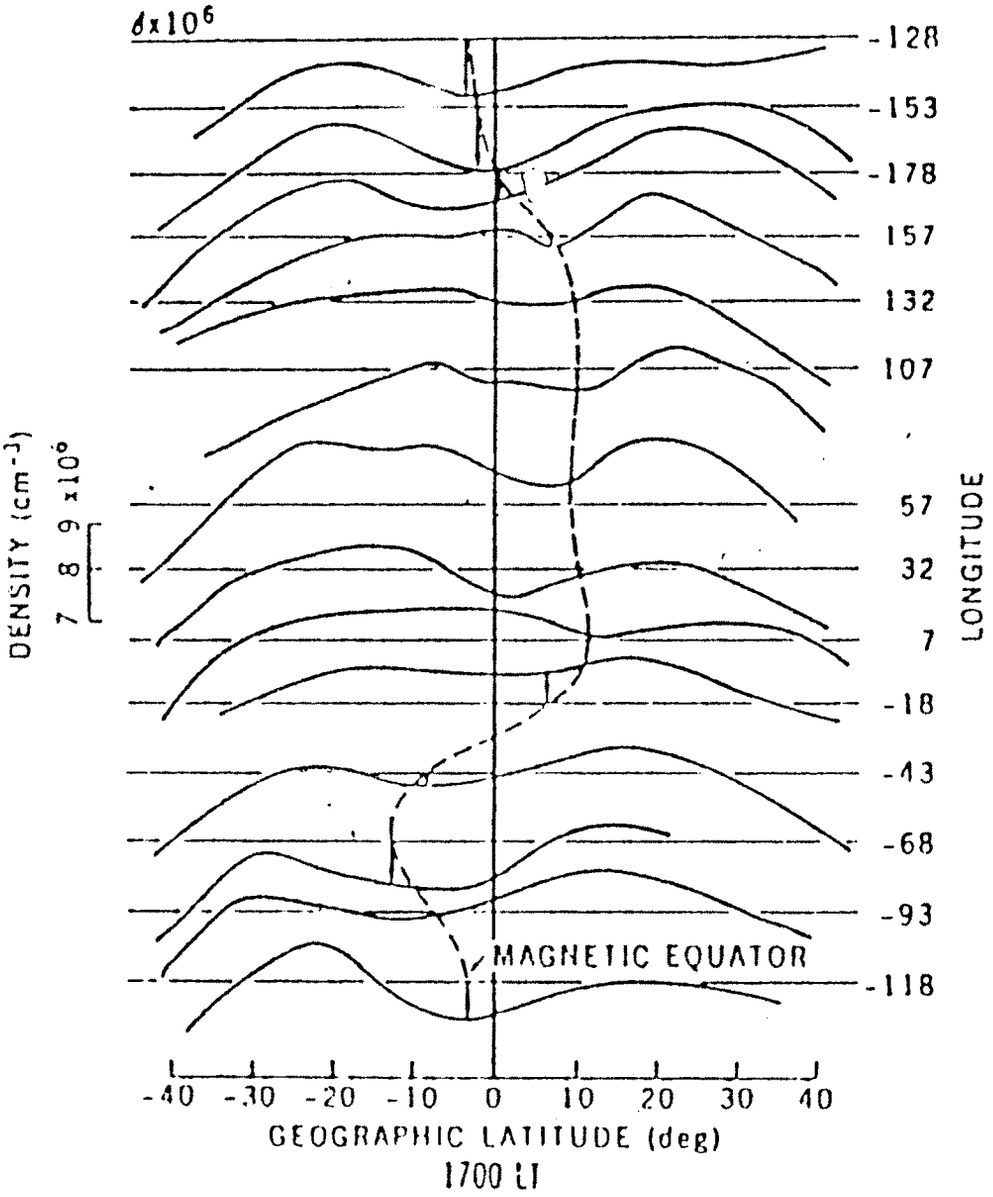

Fig. 1.11. The anomalous distribution in the N_2 densities with density crests on either side of the dip equator in the evening times.

that at the trough, offer larger resistance to the zonal wind motion that transports neutrals from the day to the nightside and thus enables its pileup at the crest location. Hence it can be seen that EIA plays an important role, not only in the redistribution of ionospheric species, but also in the latitudinal distribution of neutrals.

(F) Midnight Temperature Maximum (MTM)

There are few occasions when the measurements, both-by ground-based and satellite-borne instrumentation, revealed a pronounced increase in the neutral temperature around midnight over the equator, sometimes reaching or even exceeding the afternoon maximum temperature **[34].** This is called as Midnight Temperature Maximum (MTM). The midnight temperature maximum has been proposed by *Mayr et al.* **[35]** which arises mainly due to momentum coupling of the diurnal tide and the diurnally varying ion-drag. It can be understood by tidal theory in which transfer of energy takes place from one mode to another. The absorption of solar EUV radiation generates diurnal tide (m=1). The semi-diurnal tide (m=2) on the other hand has three major components of which the EUV has small contribution. The other two, viz., the tidal waves which originate in the lower atmosphere and the momentum coupling associated with the diurnal variations of the wind field and ion density, which are of comparable magnitude and opposite in phase, account for the large variability in the observed temperatures during midnight. The block diagram of the generation mechanism is shown in Fig-1.12 **[36].**

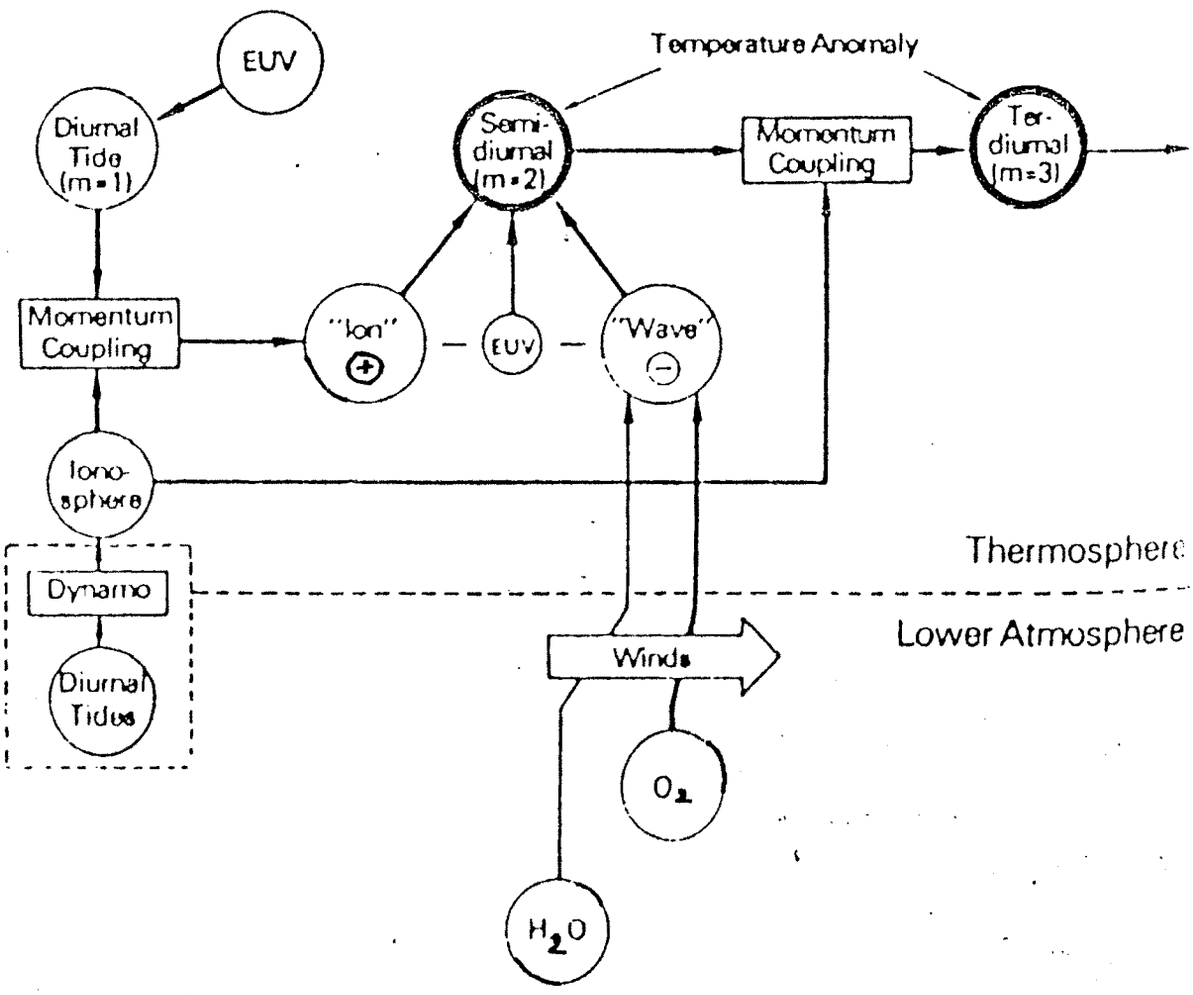

Fig. 1.12. Block diagram illustrating the processes that contribute to the midnight temperature anomaly.

(G) Equatorial Spread - F (ESF)

When the ionosphere is sounded by the radio waves, the scattering in the reflected echoes from the ionosphere in the nighttime on many occasions are observed and this phenomenon is called as Equatorial Spread-F. The Spread-F is due to the presence of about meter scale size irregularities (electron density) in the F-region. The mechanism responsible for the Spread-F is Rayleigh-Taylor instability, whose growth rate (Υ) increases non-linearly during the post sunset time under favorable background ionospheric / thermospheric conditions. The linear growth rate (Υ) is given by

$$\Upsilon = \frac{\nabla n}{n} \left(\frac{g}{\nu_{in}} + \frac{E}{B} \right) - \beta$$

Where, ∇n - is the gradient in electron density n.

ν_{in} – is the ion-neutral collision frequency .

E - is the electric field.

B - is the magnetic field.

β - is the recombination coefficient .

Rayleigh-Taylor instability occurs at the bottom of the F-region of the evening ionosphere when the plasma density gradient is anti-parallel to gravity or in other words, denser plasma is supported by lighter one. This plasma fluid type collisional Rayleigh-Taylor instability mechanism in the bottom side of the nighttime equatorial F-region causes large scale

irregularities of the order of few tens of kilometers to few hundred meters. Steeper plasma density gradient created by primary Rayleigh–Taylor mode induces other hierarchy of plasma instabilities giving rise to smaller and smaller size irregularities. These irregularities have their signature on ground-based ionograms, UHF / VHF scintillation, backscatter radar echoes, airglow depletions, etc., each depending on the scale size of irregularities. Extensive theoretical studies have been carried out towards understanding of ESF and reviewed by *Ossakow* **[37].** Simulation studies by non-linear and linear models have put forward the importance of neutral parameters such as vertically downward winds **[38],** role of topside plasma.

(H) Airglow

The ultra-violet rays of sun ionizes or dissociates the upper atmospheric gases during daytime. After withdrawal of solar rays, the dissociated and ionized products reacts amongst themselves reproducing the original species and in the process release the stored energy as radiation which manifest itself as a faint glow referred to as "airglow". A brief outline is provided here reserving the details to be discussed in chapter-2.

1.3.2 High-Latitude Phenomena

At different latitudes the energy inputs are different in origin and also in magnitudes. The particle precipitation serves energy to the high-latitude regions during magnetically quiet conditions, which is nearly equal in

magnitude with that of the solar EUV radiation over the equatorial- and low-latitudes. However, during magnetically disturbed periods the energy input can be larger by more than an order of magnitude. Almost all the high-latitude phenomena are engendered by the arrival of high-energy charged particles of solar wind origin and their interaction with the atmospheric species producing secondary and tertiary electrons, x-rays, etc. All these particles in turn dissociate and ionize the neutrals owing to collisions loosing their energy in that process which eventually heats up the upper atmosphere. The electric currents and fields are produced due to motion of charged particles. Other means of loss of the excess energy of the incoming particles are ELF/ VLF emissions, auroral hiss, optical auroral emissions, etc. Out of all the high latitude upper atmospheric phenomena, auroral emissions are the only ones, which are in visible region of the electromagnetic spectrum.

Aurora :

Aurora or 'light of the polar sky' refers to as the magnificent display of light of various seen in the upper atmospheric regions of the high-latitudes (60-70° magnetic lat.). This spectacular display is a result of various complex processes that occur in the upper atmosphere mainly due to the interaction of energetic charged particles of solar wind origin and the neutral species. The solar wind is magnetized plasma and carries with it the solar magnetic field generally known as the interplanetary magnetic field (IMF), is one of the modes in which the sun transmits its energy. It

consists of protons and electrons of high energy and is responsible for making earth's magnetic field into a comet shaped cavity called the magnetosphere, generates large amount of electric power. This power is discharged and subsequently dissipated into polar upper atmosphere/ ionosphere in various modes and their manifestations are called as "aurora". Due to availability of large amount of energies through the charged particles, which are mainly constituted by energetic electrons and protons, the auroral emissions are extremely intense as they can often be seen by even unaided eye during nighttime.One of the common picture is shown in Fig-1.13.

Specifically, auroral emissions are generated due to de-excitation of the excited species of the high-latitude upper atmosphere. The excitation itself being an outcome of energy transfer from secondary and tertiary ions engineered due to the particle precipitation. Various instruments, such as magnetometers, ionosondes, optical imagers and spectrometers, etc., both from ground and also from satellites have been used to investigate the auroral phenomena.

Though systematic photometry and high-resolution spectrometric studies are being carried out, the behavioral pattern of the aurora-related processes during daytime conditions is not yet known. There are large numbers of photochemical processes by which the excited states are produced. They are:

(1) $h\nu + A \rightarrow A^* + K.E.$ Photon impact excitation.

(2) $h\nu + A \rightarrow A^{+*} + K.E.$ Photo impact ionization and excitation.

(3) $h\nu + AB \rightarrow A^* + B^* + K.E.$ Photo dissociative excitation.

(4) $e + AB^+ \rightarrow A^* + B$ Dissociative recombination.

(5) $e^* + A \rightarrow e + A^*$ Photoelectron excitation.

(6) $e^* + A \rightarrow e + A^{+*} + e$ Photoelectron ionization excitation

(7) $e^* + AB \rightarrow e + A^* + B.$ Photoelectron impact dissociative excitation

(8) $e^* + AB \rightarrow e + A^{+*} + B^* + E$ Dissociative ionization excitation .

Where, $h\nu$ is the energy of the incident photon from the sun, A and B are atomic species, e* can represent both photoelectron and energetic electrons of solar wind origin.

The excitation processes can broadly be classified in to (1) the mutual interaction amongst the atomic species and (2) the excitation by external agencies such as solar photons and particle precipitation. The processes in first category are operative at all the time, while, some processes in the second category those due to solar photons are, obviously, operative only during the daytime. The excitation due to particle precipitation are, again, operative in both during day and nighttime as the particles of solar wind origin which enter into the earth's magnetosphere through the neutral sheet in the strong electric fields and reach the atmospheric regions along the magnetic field lines before depositing their energy **[39, 40].** The reactions involving external agencies are much more efficient as compared to those due to the atmospheric constituents alone.

A particular emission can however, be engendered by both the above mentioned processes.

1.4 Thermosphere-Ionosphere Coupling System

There exists a variety of physical and chemical processes that couples the neutral or the ionized species, behaves as a part of mutually coupled system (fig-1.14) namely, the thermospheric-ionospheric system **[36]**. Worldwide programmes such as World Ionosphere Thermosphere Study (WITS), Solar Terrestrial Energy Programme (STEP) and Coupling Energetics and Dynamics of Atmospheric Regions (CEDAR) have been initiated to understand the various complex processes, all of which finally end up in the transfer of energy and momentum to and between the ions and neutrals. The satellite missions like OGO series, Atmosphere Explorer Series, etc. showed the physical, chemical and dynamical processes pertaining to the upper atmosphere. The chemical, fluid dynamical and electrodynamical properties of the system are associated with coupling of the thermosphere and the ionosphere. The basic interaction mechanisms are as follows.

(1)Chemistry: Though the peak production of ionization is below 200 km, the plasma density increases with altitude due to the role of ion chemistry. By the radiative recombination with the ambient electron, the O^+ ion is neutralized or by the charge exchange reaction with the molecular species which eventually dissociatively recombine with the ambient electrons. The former is an extremely slow process with reaction rate of 10^{-12} cm^3s^{-1} at

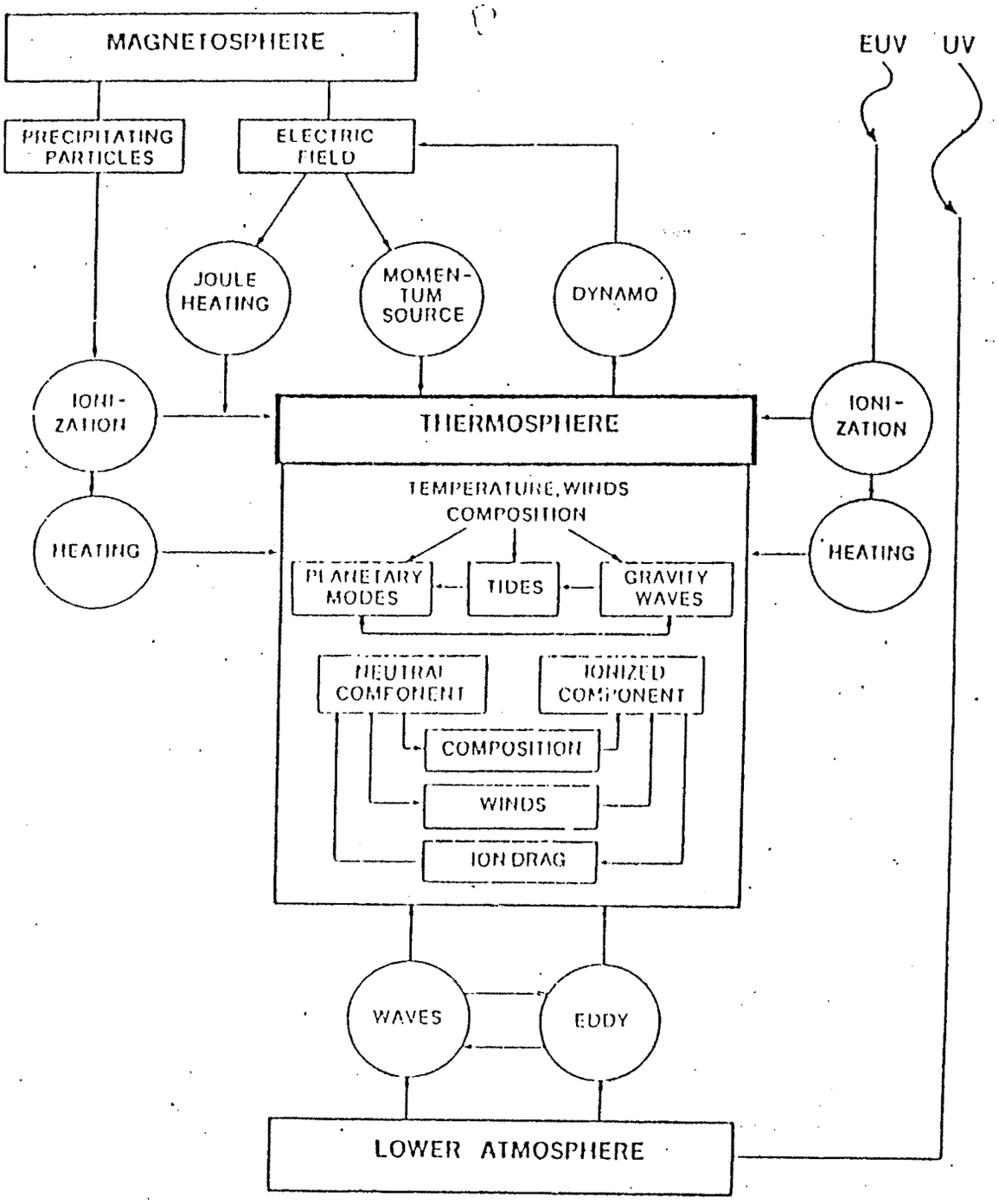

Fig. 1.14 Schematic block diagram of thermospheric-ionospheric coupling system.

least two orders of magnitude slower than the latter reaction **[41]**. The loss of O^+ here is by a two-stage process. O^+ ions undergo ion-atom interchange (*charge-exchange*) reaction with O_2 and N_2 to give O_2^+ and NO^+ **[42]**.

$$O^+ + O_2 \xrightarrow{k1} O^+_2 + O$$

$$O^+ + N_2 \xrightarrow{k2} NO^+ + N$$

k1 and k2 are their respective charge exchange rates.

The molecular ions so formed are lost by dissociative recombination to become neutral species.

$$O_2^+ + e \xrightarrow{\alpha 1} O + O^+$$

$$NO^+ + e \xrightarrow{\alpha 2} O + N$$

Due to the declining molecular densities, O^+ ions can sustain for long duration (even days) at the F-region altitudes. Under the equilibrium conditions, the production rate "q" is given by:

$$\frac{1}{q} = \frac{1}{\alpha N^2} + \frac{1}{\beta N}$$

Where, N is the electron density which is equal to the sum of the all atomic and molecular ions: $\sum N_i = N^+_A + N^+_M = N$, and $\beta = k[M]$, [M] being the molecular concentration. The two limiting cases of this reaction are :

$q = \alpha N^2$ if $\beta >> \alpha N$, i.e., molecular ions >> atomic ions .

And, $q = \beta N$, if $\beta << \alpha N$, i.e., atomic ions >> molecular ions.

In the E- and lower F-regions, the concentration of molecular ions is much larger than the atomic ions. The dissociative recombination reaction

governs the loss of ionization and hence the formula $q = \alpha N^2$ (square law loss rate) holds, while in the upper F-region, atomic ions are dominant and charge-exchange reaction controls the loss rate of electrons and hence, $q=\beta N$ (linear loss rate) is applicable. In the transition region around 160 to 200 km both the processes are operative. When this transition region happens to coincide with the height of peak production of the F-layer, a splitting of the F-layer, into F_1 and F_2 takes place during local noontime. As the recombination rate falls off more rapidly with altitude than the ionization rate, larger ion concentration occurs at altitudes above F_1–layer. Above the F_2 –layer, however, downward diffusion of ions along the magnetic field lines is faster than either the rate of ionization or the rate of recombination and causes the ion concentration to decrease with altitude. During nighttime F_1-and F_2-layer merge into a single one. In the F-region the motion of both ion and electron is governed by the geomagnetic field lines with their gyrofrequencies are higher than their respective collision frequencies with neutrals.

At 100 km, lifetime of O^+ is about few-seconds which increases to the orders of days in the upper ionosphere. After sunset, in the absence of any further production, the E-region where molecular ions dominate, disappears mainly due to the faster recombination process. However, the ionization in the F-region is retained all through the night due to the long-lived atomic ions O^+. In this region, transport processes, namely, diffusion and plasma drifts compete with the loss processes to take control of the

behavior of the entire F-layer.

Most of the ionospheric parameters discussed above have been inferred from ground-based instruments, while the neutral parameters, such as densities, temperature etc., have been accurately determined by in-situ measurements by instruments on-board rocket and satellites. It was *Jacchia* **[43]** who first used the satellite-drag information to infer the overall densities and temperatures of the upper atmosphere paving the way for the formulation of atmospheric model.

A change in the loss coefficient is affected by several ways **[44],** changes in the ratio of molecular to atomic concentration of neutral air is one of them. Further, the loss coefficient is a sensitive parameter of neutral temperature and it changes through the temperature dependence of the reaction rate coefficients and molecular concentration.

(2) Diffusion

The vertical diffusion of plasma through the ambient neutral atmosphere depends on the ion-neutral atmosphere on the ion-neutral collision frequency and it is expected to control the behavior of the ionospheric layer at very high altitudes. The diffusion is of ambipolar type, i.e., the ions and electrons diffuse together, and any separation between them is nullified by the presence of an electric field, which results in movements of both ion and electrons. The motion of ions and electrons is governed by the geomagnetic field and their diffusion varies with the dip angle. In terms of the dip angle I, the vertical diffusion coefficient is $D \sin^2 I$.

Since over the dip equator the magnetic field lines are horizontal in the north-south direction, the vertical diffusion process of ions and electrons becomes unimportant. The diffusion coefficient 'D' depends on neutral atmospheric densities through its dependence on the ion-neutral collision frequency.

The interplay of the chemical and plasma diffusion processes controls the dynamic F- region. The F_2-layer can be moved by wind or electric fields to altitudes where the recombination and diffusion coefficients are different, and the plasma density distribution would vary accordingly. When F_2 –region moves downward loss is enhanced and peak density N_mF_2 decreases and the reverse is true when the F-region moves upward. This mechanism was proposed initially for midlatitudes where the large dip angle of the magnetic field lines aids diffusion in the vertical direction **[45, 46]**, which is essentially formed the basis of the servo principle of F-region.

(3) Winds

The diurnal cooling and heating of the thermosphere generate horizontal gradients in pressure that drives neutral air circulation. There are many effects of winds on the ionosphere. The neutral wind in the north-south meridian plane induces vertical motion to the F-layer along the magnetic field lines. The vertical plasma velocity is given by:

$$\upsilon_z = U \sin I \cos I.$$

An equatoward wind will push the plasma upward while a poleward wind would force it downward. The zonal motion of ions across the magnetic field produced by the zonal component of neutral wind leads to generation of dynamo in the E- and F-regions. The ionosphere parameters such as plasma drifts, electric fields, as well as the height distribution of plasma density, are governed to large extent by the magnitude and direction of neutral winds.

(4) Ion-drag

For the thermally driven wind system the ion-drag is the major force that limits the wind velocity and sets the neutral motion across the isobars. It was *Geisler* **[47],** who first derived a thermospheric wind system allowing for the decrease of ionization and hence the ion-drag from day to night. At night equatoward motion was found to be stronger than the daytime poleward motion, showing the day-to-night variation of ion-drag. *Rishbeth* **[48],** showed the effects of ion-drag on the neutral atmosphere and its motion in the equatorial region. The poleward wind brings the F-layer down enhancing the ion-drag force and the zonal components of the wind gets reduced in magnitude. This mechanism is effective in nighttime when F-layer is relatively thin compared to that during daytime. The neutral wind thus becomes sensitive to the vertical movement of the F-layer **[49].**

(5) Electric Fields

The plasma in the F-region undergoes an **E** × **B** drift, in the presence of an eastward electric field. The fountain effect is responsible for the equatorial ionization anomaly **[50].** Further, the electric field is one of the factors that triggers plasma instabilities in the nighttime equatorial F-region that in turn generates a wide spectrum of irregularities referred to as equatorial spread-F (ESF) **[51, 52].**

1.5 Outline of the Present Work

The Chapter-1 starts with introductory part regarding the structure of the earth's upper atmosphere. Various phenomena that are prevalent in equatorial -and low-latitude as well as high-latitudes are briefly reviewed. An attempt is also made to highlight the coupling between the thermosphere and ionosphere.

The relative theoretical background of airglow emissions such as origin of airglow , classification of airglow , photochemical process in the ionosphere and theory of emission of OI 630 nm and OI 557.7 nm night airglow in particular is presented in Chapter-2

Chapter-3 deals with the ionospheric modeling and thermospheric modeling studies.

Chapter-4 describes the detail construction and working of ground based instrumentation to probe the upper atmosphere.

Chapter-5 presents data analysis. In this section we present

the correlation between optical data, ionospheric data and geomagnetic data.

Chapter-6 deals with summary and conclusion.

REFERENCES

1. Hedin, A.E., MSIS-86 thermospheric model, *J. Geophys. Res.*, **92**, 4649-4662, 1987.
2. Bates, D.R., Formation of the ionized layers, solar eclipses and the ionosphere, edited by W.S.G. Beynon and G.M. Brown, *Pergamon Press London*, 184-188, 1956.
3. Stolarski, R.S., P.B. Hays and R.G. Roble, Atmospheric heating by solar EUV radiation, *J. Geophys. Res.*, 80, 2266, 1975.
4. Dickinson, R.E., R.G. Roble and E.C. Ridley, Response of the neutral thermosphere at F-layer heights to interaction of a global wind with anomalies of ionization, *J. Atmos. Sci.*, **28**, 1280, 1971.
5. Tinsley, B.A., Neutral atom precipitation. *A review, J. Atoms. Terr. Phys.*, **43**, 617, 1981.
6. Prolss, G.W., M. Roemer and J.W. Slowey, Dissipation of solar wind energy in the earth's upper atmosphere: The geomagnetic effect, *Adv. Space Res.*, **8**, (5), 215, 1988.
7. Hines, C.O., Dynamical heating of the upper atmosphere, *J. Geophys. Res.*, **70**, 177, 1965.
8. Chapman, S. and R.S. Lindzen, Atmospheric Tides, D. Reidel, Dordrecht, 1970.
9. Richmond, A.D., Large-amplitude gravity wave energy production and dissipation in the thermosphere, *J. Geophys. Res.*, **84**, 1880, 1979.

10. Cole, K.D. and M.P. Hickey, Energy transfer by gravity wave dissipation, *Adv. Space Res.*, **1**, (12), 65, 1981.

11. Killeen, T.L., Energetics and dynamics of the earth's thermosphere, *Rev. Geophys.*, **25**, 433, 1987.

12. Cole, K.D., Joule heating of the upper atmosphere, *Australian J. Phys.*, **15**, 223-235, 1962.

13. Stewart, B., *Encyclopedia Britannica, 9th Ed.*, **16**, 181, 1882.

14. Sampath, S., and T. S. G. Sastri, Results from in-situ measurements of ionospheric currents in the equatorial region-I, *J. Geomag. Geoelectr.*, **31**, 373-379, 1979.

15. Gouin, P., Reversal of the magnetic daily variation at Addis Ababa, *Nature*, **193**, 1145-1146, 1962.

16. Rastogi, R. G., Counter equatorial electrojet currents in the Indian zone, *Planet. Space.* Sci., **21**, 1355-1365, 1973.

17 Kane, R.P., Geomagnetic field variations, *Sci. Space Rev.*, **18**, 413-540, 1975.

18. Raghavarao, R., B.G. Anandarao, Vertical winds as a plausible cause for equatorial counter electrojet, *Geophys. Res. Lett.*, **7**, 357-360, 1980.

19. Anandrao, B.G. and R. Raghavarao, Structural changes in the currents and fields of the equatorial electrojet due to zonal and meridional winds, *J. Geophys. Res.*, **92**, 2514-2526, 1987.

20. Croom, S. A. Robbins, and J. O. Thomas, Two anomalies in the

behaviour of the F_2 layer of the ionosphere, *Nature*, **184**, 2003-2004, 1959.

21. Rao , C.S.R., and P.L. Malhotra. A study of geomagnetic anomaly during I.G.Y.,*J. Atoms . Terr. Phys.*, **A26**, 1075-1085, 1964.

22. Sivaraman, M.R., R. Suhasini and R. Raghavarao, Role of ambipolar diffusion in the development of equatorial anomaly in solar maximum and minimum period , *Ind. J. Radio Space Phys.*, **5**, 136-144, 1976.

23. Rastogi, R.G., and J.A. Klobuchar, Ionospheric electron content within the equatorial F_2 layer anomaly belt, *J. Geophys. Res.*, **95**, 19045-19052, 1990.

24. Walker, G.O., J.H.K. Ma and E. Gotton, The equatorial ionosphere anomaly in electron content from solar minimum to solar maximum from South-East Asia, *Ann. Geophysicae*, **12**, 195-209, 1994.

25. Lyon, A.J., and L. Thomas, The F_2-region equatorial anomaly in the African, American and East Asian sectors during sunspot maximum, *J. Atoms. Terr. Phys.*, **25**, 373-386, 1963.

26. Lockwood, G.E.K., and G.L. Nelms, Topside sounder observations of the equatorial anomaly in the 75° W longitude zone, *J. Atoms. Terr. Phys.*, **26**, 569-580, 1964.

27. Walker, G.O., J.H.H. Ma, R.G. Rastogi, M.R. Deshpande and H. Chandra, Dissimilar forms of the ionospheric equatorial anomaly observed in East Asia and India, *J. Atoms. Terr. Phys.*, **42**, 629-635,

1980.

28. Sharma, P. and R. Raghavarao, Simultaneous occurrence of ionization ledge and counter-electrojet in the equatorial ionosphere: observational evidence and its implications, *Can. J. Phys.*, **67**, 166, 1989.

29. Raghavarao, R., P. Sharma and M.R. Sivaraman, Correlation of Ionization anomaly with the intensity of the electrojet, *Space Res.*, ***XVIii***, 277-280, 1978.

30. Raghavarao, R., R. Sridharan, J.H. Sastri, V.V. Agashe, B.C.N. Rao, P.B. Rao and V.V. Somayajulu, The equatorial ionosphere, World Ionospheric/ Thermospheric Study, *WITS Handbook,.Vol.**1***, p.48, 1988a.

31. Sastri, J. H., Equatorial anomaly in F-region – *A review, Indian J. Radio Space Phys.,* **19**, 225, 1990.

32. Abdu, M.A., J.H.A. Sobral, E.R. De Paula and I.S. Batista, Magnetospheric disturbance effects on the equatorial ionization anomaly (EIA): an overview, *J. Atoms.Terr. Phys.*, **53**, 757-771, 1991.

33. Hedin, A.E. and H.G. Mayr, Magnetic control of the near equatorial neutral thermosphere, *J. Geophys. Res.*, **78**,1688, 1973.

34. Spencer et al., The midnight temperature maximum in the earth's equatorial thermosphere, *Geophys . Res. Lett.*, **6**, 444, 1979.

35. Mayr et al., Tides and the midnight temperature anomaly in the

thermosphere, *Geophys. Res. Lett.*, **6**, 447, 1979.

36. Mayr, H.G., I. Harris and N.W. Spencer, Some properties of upper atmosphere dynamics, *Rev. G eohpys. Space Phys.*, **16**, 539, 1978.

37. Ossakow, S.L., Spread-F theories- A review, *J. Atoms. Terr. Phys.*, **43**, 437-452, 1881.

38. Sekar, R. and Raghavarao, Role of vertical winds on the Rayleigh-Taylor mode instabilities of the nighttime equatorial ionosphere, *J. Atoms. Terr. Phys.*, **49**, 981, 1987.

39. Akasofu, S. I., The solar wind magnetosphere energy coupling and magnetospheric disturbances, *Planet. Space Sci.*,**28**, 495 - 509, 1980.

40. Arnoldy, R. L., Review of partical precipitation physics of auroral arc formation, edited by S.I. Akasofu and J.R. Kan, *American Geophysical union*, Washington, 56-66,1988.

41. Banks, P. M. and G. Kockarts, *Aeronomy*, Academic Press , New York, 1973.

42. Bates, D. R., Charge transfer and ion-atom interchange collisions, *Proc. Phys. So. London*, **A68**, 344-345, 1955.

43. Jacchia, L. G., Static diffusion models of the upper atmosphere with empirical temperature profiles, *Smithson Contrib. Astrophys.*, **8**, 215, 1965.

44. Rishbeth, H., On the F_2 layer continuity equation, *J. Atoms. Terr. Phys.*, **48**, 511, 1986.

45. Rishbeth, H., The effect of winds on the ionospheric F_2 peak, *J. Atoms. Terr. Phys.*, **29**, 225, 1967.

46. Rishbeth, H., S. Ganguly and J.C.G. Walker, Field - aligned and field –perpendicular velocities in the ionospheric F_2 -layer, *Atoms. Terr. Phys.*, **40**, 767, 1978.

47. Geisler, J.E., A numerical study of the wind system in the middle thermosphere, *J. Atoms. Terr. Phys.*, **29**, 1469, 1967.

48. Rishbeth, H., Ion-drag effect in the thermosphere, *J. Atoms. Terr. Phys.*, **41**, 885, 1979.

49. Forbes, J. M. and R. G. Roble, Thermosphere-Ionosphere Coupling: An experiment in interactive modeling, *J. Geophys. Res.*, **95**, 201, 1990.

50. Hanson, W.B. and R.J. Moffett, Ionization transport effects in the equatorial F-region, J. Geophys. Res., **71**, 5559, 1966.

51. Fejer, B.G. and M.C. Kelley, Ionospheric irregularities, *Rev. Geophys. Space Phys.*, **18**, 401, 1980.

52. Hanson, W.B., B.L. Cragin and A. Dennis, The effect of vertical drift on the equatorial F-region stability, *J. Atoms. Terr. Phys.*, **48**, 205, 1986.